Published in final edited form as:

Biochemistry. 1979 February 06; 18(3): 508–519. doi:10.1021/bi00570a021.

Differential Polarized Phase Fluorometric Investigations of Diphenylhexatriene in Lipid Bilayers. Quantitation of Hindered Depolarizing Rotations

J. R. Lakowicz, **F. G. Prendergast**, **D. Hogen**

Department of Biochemistry and Freshwater Biological Institute, University of Minnesota, Navarre, Minnesota 55392 (J.R.L. and D.H.), and the Department of Pharmacology, Mayo Medical School, Rochester, Minnesota 55901 (F.G.P.).

Abstract

Differential polarized phase fluorometry has been used to investigate the depolarizing rotations of 1,6-diphenyl-1,3,5-hexatriene (DPH) in isotropic solvents and in lipid bilayers. For DPH dissolved in isotropic solvents, there is a precise agreement between the observed and predicted values for maximum differential tangents, indicating that in these media DPH is a free isotropic rotator. In lipid bilayers the tangent defects (i.e., the differences between the calculated and the observed maximum differential tangents) are too large to be explained by anisotropy in the depolarizing rotations but are accounted for by hindered isotropic torsional motions for the fluorophore [Weber, G. (1978) *Acta Phys. Pol. A 54*,173.]. This theory describes the depolarizing rotations of the fluorophore by its rotational rate R (in radians/second) and the limiting fluorescence anisotropy (r_∞) at times long compared with the fluorescence lifetime. Through the combined use of both steady-state anisotropy measurements and differential phase measurements, we have demonstrated that one may obtain unique solutions for both R and r_∞. For DPH embedded in vesicles prepared from dimyristoyl-, dipalmitoyl-, and distearoylphosphatidylcholines, the depolarizing motions are highly hindered at temperatures below the transition temperature (T_c) but are unhindered above T_c. The apparent rotational rates of the probe do not change significantly at T_c. These data suggest that the changes observed in the steady-state anisotropy near T_c derive primarily from changes in the degree to which the probe's rotations are hindered, and only to a small extent from changes in rotational rate. For DPH embedded in bilayers that contained 25 mol % cholesterol, no clear transition occurred and the rotations appeared to be hindered at all temperatures. The rotational motions of DPH embedded in dioleoylphosphatidylcholine were found to be far less hindered, but the rotational rates were similar to those obtained in the saturated phosphatidylcholines. Finally, the data show that in an anisotropic environment, such as that of a lipid bilayer, steady-state fluorescence anisotropy measurements alone cannot yield quantitatively meaningful rotational rates. Extrapolation of steady-state anisotropy data to the quantitation of membrane viscosity is therefore difficult, if not invalid; however, qualitative comparisons can be useful.

In the present work we use differential polarized phase fluorometry to investigate the depolarizing rotations of the 1,6-diphenyl-1,3,5-hexatriene (DPH)[1] in isotropic solvents and

[1]Abbreviations used: DPH, 1,6-diphenyl-1,3,5-hexatriene; DMPC, DPPC, DSPC, DOPC, dimyristoyl-, dipalmitoyl-, distearoyl-, and dioleoyl-L-α-phosphatidylcholine, respectively; CHOL, cholesterol; DPPC-E, dipalmitoyl ether-L- α -phosphatidylcholine.

in lipid bilayers. Fluorescence anisotropy measurements provide a measure of the rotational diffusion of fluorophores. The rate of rotation is thought to reflect the viscous drag imposed by the fluorophore's immediate environment. As a result, measurements of steady-state fluorescence anisotropies have been frequently used to estimate the microviscosity of lipid bilayers in which the fluorophores are located (Cogen et ai., 1973; Shinitzky et al., l971). DPH has become widely used in studies of this type because of its favorable spectral properties (Shinitzky & Barenholz, 1974), but perhaps most importantly because of the large changes in fluorescence anisotropy that occur at the membrane transition temperature (Lentz et al., 1976a,b). The central assumption of these estimates of membrane microviscosity is that the isotropy and freedom of the depolarizing rotations of the fluorophore in the lipid bilayer are identical with those in an isotropic reference solvent. Recent time-resolved anisotropy studies of DPH in lipid bilayers have indicated that the main assumption upon which microviscosity measurements are predicated may be invalid (Chen et al., 1977; Kawato et al., 1977; Dale et al., 1977; Kinosita et al., 1977). We have also examined this issue, using a completely different technique, namely, differential polarized phase fluorometry. In this technique one measures the difference in lifetime between the parallel and perpendicular components of the fluorescence emission when the sample is excited by vertically polarized, sinusoidally modulated light. The theoretical basis for the measurements was developed by Weber (1977) and used by Mantulin & Weber (1977) to examine anisotropic fluorophore rotations in homogeneous solutions. More recently the theory was extended to fluorophores in a hindered environment (Weber, 1978), and we (Lakowicz & Prendergast, 1978a) developed a method to obtain unique solutions for the probe's rotational rate (R) and the degree to which these rotations are hindered (r_∞). The present paper provides a detailed discussion of the technique and extensive data and data analysis of the rotational motions of DPH in solvents and lipid bilayers.

Theory

The technique of differential polarized phase fluorometry is still sufficiently unfamiliar that the relevant aspects of and some of the manipulations necessary to apply the theory to our data are discussed in some detail below.

After pulsed excitation with vertically polarized light, the decays of fluorescence intensity of the parallel ($I_\parallel(t)$) and perpendicular ($I_\perp(t)$) components of the fluorescence emission are known to be doubly exponential (Jablonski, 1957, 1965; Weber, 1979; Perrin, 1936). In particular these components are

$$I_\parallel(t) = \frac{1}{3}e^{-t/\tau} + \frac{2}{3}r_0 e^{-(1/\tau + 6R)t} \tag{1}$$

$$I_\perp(t) = \frac{1}{3}e^{-t/\tau} - \frac{1}{3}r_0 e^{-(1/\tau + 6R)t} \tag{2}$$

where r_0 is the fluorescence anisotropy observed in the absence of depolarizing rotations, R is the rotational rate in radians per second, and τ is the fluorescence lifetime. From these

equations it is easily noted that a polarizer oriented to transmit 33.3% of the parallel component and 66.7% of the perpendicular component (54. 7° from the vertical) effectively removes from observation those components due to fluorophore rotation. Steady-state anisotropy measurements correspond to integration of the time response function over times from zero to infinity. Hence the steady-state parallel and perpendicular intensities are given by

$$I_{\|} = (1/\tau)\int_0^{\infty} I_{\|}(t)\mathrm{d}t \tag{3}$$

$$I_{\perp} = (1/\tau)\int_0^{\infty} I_{\perp}(t)\mathrm{d}t \tag{4}$$

Using this approach one readily obtains the Perrin equation

$$r_0/r = 1 + 6R\tau \tag{5}$$

where r is the fluorescence anisotropy in the presence of depolarizing rotations and is given by

$$r = \left(I_{\|} - I_{\perp}\right)/\left(I_{\|} + 2I_{\perp}\right) \tag{6}$$

An intuitive presentation of a differential polarized phase fluorometer is given in Figure 1. Detailed schematic diagrams have been presented elsewhere (Mantulin & Weber, 1977; Lakowicz & Prendergast, 1978b). The exciting light is polarized vertically and modulated sinusoidally at either 10 or 30 M Hz. The fluorescence emission is observed through a polarizer and is referenced to the parallel component observed by the right-hand channel. Differences in phase angle between the parallel and perpendicular components of the emission are observed by rotation of the left polarizer by 90°. The phase angle of the perpendicular component of the emission is larger than that of the parallel component since the fluorophore must rotate into this new plane of observation in order to be observed through the perpendicular polarizer. The parallel phase angle is smaller than the perpendicular phase angle because the parallel polarizer selects those molecules which have emitted a photon prior to significant rotation. A phase shift between these components is only observed when the parallel and perpendicular populations are exchanging on a time scale comparable to the fluorescence lifetime (Weber, 1977; Jablonski, 1957). When the rotations are much faster than the emission, or when the fluorophores are fixed, no phase shift is predicted or observed. Differential phase angles will be presented as the tangent of this angle (tan Δ). This quantity is related to the difference in lifetime between the parallel and perpendicular components ($\Delta\tau$) by

$$\tan\Delta = \omega\Delta\tau \tag{7}$$

where ω is the circular modulation frequency. Clearly we wish to determine tan Δ under different conditions (say of varying temperature) and relate these to rotational rates of the probe.

The tangent of the phase angle between the parallel and perpendicular components of the fluorescence emission is a function of R, r_0, τ, and ω. For an unhindered isotropic rotator tan Δ is given by (Weber, 1977)

$$\tan\Delta = \frac{(2R\tau)\omega\tau r_0}{\frac{1}{9}m_0\left(1+\omega^2\tau^2\right)+\frac{(2R\tau)}{3}\left(2+r_0\right)+(2R\tau)^2} \tag{8}$$

Where

$$m_0 = \left(1+2r_0\right)\left(1-r_0\right) \tag{9}$$

The quadratic form of eq 8 may be used to obtain R from measurements of tan Δ and τ.

$$(2R\tau)^2+(2R\tau)\left[\frac{2+r_0}{3}-\left|\frac{r_0}{\tan\Delta}\right|\omega\tau\right]+ (1/9)m_0\left(1+\omega^2\tau^2\right)=0 \tag{10}$$

In general the correct value of R is chosen from the temperature dependence of R, or from a comparison between R values obtained from tan Δ measurements with those obtained from eq 5. For a free isotropic rotator we expect precise agreement for rotational rates obtained by these two methods.

For isotropic depolarizing rotations, the maximum value of tan Δ (tan Δ_{max}) is a function Of Only r_0, ω, and τ.

$$\tan\Delta_{max} = \frac{3\omega\tau r_0}{\left(2+r_0\right)+2\left[m_0\left(1+\omega^2\tau^2\right)\right]^{1/2}} \tag{11}$$

The studies of Mantulin & Weber (1977) clearly demonstrate that anisotropic rotations can be detected by tan Δ_{max} values which are less than predicted by eq 11. Tangent defects can also result from a heterogeneous population of isotropic rotators or from hindered torsional motions of the fluorophore.

Initial experiments with DPH in lipid bilayers revealed tangent defects which were too large to be explained by rotational anisotropy (Weber, 1977). In addition, we expected (1) the depolarizing rotations of DPH to be isotropic (Shinitzky & Barenholz, 1974; rotations of DPH along an axis parallel to its long axis do not displace the electric dipole and therefore do not result in depolarization) and (2) DPH to be in a volume-restricted but at least moderately homogeneous environment. We speculated that this probe might exhibit isotropic but hindered torsional motions.

Recently Weber (1978) modified eq 1 and 2 to allow for a nonzero limiting anisotropy (r_∞) at times which are long compared with the fluorescence lifetime.

$$I_{\parallel}(t) = (1/3)\left(1 + 2r_\infty\right)e^{-t/\tau} + (2/3)\left(r_0 - r_\infty\right)e^{-(1/\tau + 6R)t} \tag{12}$$

$$I_{\perp}(t) = (1/3)\left(1 - r_\infty\right)e^{-t/\tau} - (1/3)\left(r_0 - r_\infty\right)e^{-(1/\tau + 6R)t} \tag{13}$$

By integration and normalization of these equations over times from zero to infinity, we obtain

$$r_\infty = r + \left(r - r_0\right)/6R\tau \tag{14}$$

Weber (1978) obtained tan Δ for an isotropic hindered rotator

$$\tan\Delta = \frac{\omega\tau\left(r_0 - r_\infty\right)(2R\tau)}{\frac{1}{9}m_0\left(1 + \omega^2\tau^2\right) + \frac{1}{3}S(2R\tau) + m_\infty(2R\tau)^2} \tag{15}$$

where

$$\begin{aligned} m_\infty &= (1 + 2r_\infty)(1 - r_\infty) \\ S &= 2 + r_0 - r_\infty(4r_0 - 1) \end{aligned} \tag{16}$$

The maximum value of tan Δ is given by

$$\tan\Delta_{\max} = \frac{3\omega\tau\left(r_0 - r_\infty\right)}{S + 2\left[m_0 m_\infty\left(1 + \omega^2\tau^2\right)\right]^{1/2}} \tag{17}$$

For $r_\infty = 0$, eq 15 and 17 reduce to those applicable to an unhindered isotropic rotator (eq 8 and 11). In lipid bilayers the maximum observed tan Δ occurs near the transition temperature. A priori, we do not know how rapidly R and r_∞ are changing with temperature, but it is clear that both may change. Examination of eq 15 shows that a maximum tan Δ can result from either a changing R or r_∞. As a result this equation cannot be used to determine either variable. Equation 17 is only applicable when r_∞ is a constant. Thus differential phase measurements alone do not allow R and r_∞ to be obtained for a fluorophore in a hindered environment; yet it would be of obvious value to have these quantities since each provides information on the motional freedom of the fluorophore. We recognized that one could combine differential phase measurements with steady-state anisotropy measurements to obtain unique solutions for R and r_∞.

By substitution of eq 14 into eq 15, we obtain

$$(m\tan\Delta)(2R\tau)^2 + (C\tan\Delta - A)(2R\tau) + (D\tan\Delta - B) = 0 \quad (18)$$

where

$$A = 3B = \omega\tau(r_0 - r)$$
$$C = (1/3)(2r - 4r^2 + 2)$$
$$D = (1/9)(m + m_0\omega^2\tau^2)$$
$$m = (1 + 2r)(1 - r)$$

Hence measurement of r, tan Δ, and τ allows R to be obtained from eq 18. Generally one of the two possible values of R was negative and therefore inadmissible. The calculated value of R is then substituted in eq 14, along with the steady-state anisotropy to obtain r_∞.

Materials and Methods

The diacylphosphatidylcholines were all obtained from Sigma Chemicals. The dipalmitoyl ether analogue of dipalmitoylphosphatidylcholine was obtained from Serdary Research Laboratories, Inc., London, Ontario, Canada. These phospholipids migrated as a single spot on silica using chloroform:methanol:water (65:25:4) as the solvent DPH was obtained from Aldrich. Propylene glycol was obtained from Eastman, and mineral oil was obtained from Weber and Judd, Co., Rochester, MN. In all cases the background fluorescence from unlabeled lipids or from solvents was less than 1% of the total intensity. All other chemicals used were reagent grade.

Phospholipid vesicles were prepared as follows: to a stainless steel beaker was added a known amount of phospholipid dissolved in benzene. An aliquot of a freshly prepared solution of DPH in benzene was then added to yield a molar ratio of lipid to DPH of 500:1. The benzene was removed by evaporation under a flow of dry argon or nitrogen while the beaker was partially immersed in a water bath maintained at about 50 °C. This treatment was continued for 30 min after the sample appeared to be solvent free. Buffer (0.05 M KCl, 0.01 M Tris, pH 7.5) was added to yield final lipid concentration of 0.17 mg/mL. The lipid buffer mixture was then sonicated with a Heat Systems Model 350 sonicator (set at 200 W) for about 15 min under a nitrogen atmosphere. During sonication the temperature was about 10 °C above the transition temperature. Sonicated samples were than annealed for 30 min at a temperature of at least 10 °C above T_c (Lawaczeck et al., 1976) and finally centrifuged at the same temperature at 48 000g for 1 h. The supernatant was used for subsequent experiments without further treatment. Multilamellar liposomes were prepared by vigorously shaking a test tube containing a film of dried lipid and buffer. Phosphate analysis of the final solutions indicated that the actual phospholipid concentrations were within 10% of the expected value.

Measurements of Differential Tangents, Fluorescence Lifetimes, and Steady-State Anisotropies.

Fluorescence measurements were made on an SLM subnanosecond fluorometer operated in the T format as shown in Figure 1. The sample is placed in a thermostated sample holder and exposed to light, the amplitude of which is modulated by a Debye-Sears modulator. The exciting light is polarized in the vertical direction by a Glan-Thompson polarizer. The phase angles between the parallel and perpendicular components of the fluorescence emission are measured in the following manner (see Figure 1). First the phase difference is determined with the left polarizer in the horizontal position and the right polarizer aligned vertically. This measurement contains both the phase shift due to the rotation of the fluorophore and the shift resulting from instrumental factors. The left polarizer is then rotated to the vertical orientation; the phase angle is remeasured and subtracted from the previous reading. With both polarizers vertical, the phase angles are identical; as a result, the second reading contains only the phase shift resulting from instrumental factors. The right-hand polarizer may be left in either the vertical position, as shown. or in the horizontal orientation. Identical differential tangents are obtained, which is to be expected since the left channel serves only as a phase reference point.

The photoelectron transit time through a photomultiplier is known to be dependent upon the region of the photocathode from which it originates. Any change in the image location of a signal on the photocathode can alter the time response of a photomultiplier and thus alter the phase angles. Rotation of the emission polarizer could result in a movement of the image. We tested this possibility by setting the excitation polarizer in the horizontal orientation. Under these conditions we expect tan $\Delta = 0$ since both emission channels observe a perpendicular component of the emission, regardless of their orientation. The observed tan Δ values with the exciting polarizer horizontal were always within experimental limits of zero.

Fluorescence lifetimes were obtained by observation of the phase shift of the fluorescence emission of the samples relative to that of a glycogen-scattering solution (Spencer & Weber, 1 969). For these measurements the instrument was phase referenced to the signal going to the Debye-Sears modulator. The errors in τ are about fivefold larger than the errors in $\Delta\tau$, since the former was determined by a nondifferential method. The excitation polarizer was in the vertical position, and the emission polarizer set at 54.7°. This angle was obtained by observing the polarizer position where the scattered light intensity of the glycogen solution is 33% of the maximum intensity (the latter occurs when this polarizer is in the vertical position). The use of these polarizer orientations eliminates the effects of depolarizing rotation on the observed fluorescence lifetime (Spencer & Weber, 1970).

Steady-state fluorescence anisotropy measurements were made directly in the differential phase fluorometer with the light modulation and radio frequency electronics were turned off. We routinely varied the exciting polarizer to measure *r*, but identical results were obtained by variation of the; emission polarizer, as is done in measurements of $\Delta\tau$ (i.e:, of tan Δ).

In all these measurements the following instrumental conditions were utilized: exciting wavelength, 360 nm; exciting filter, Corning 7–54; emission filters, 2 mm of 1 M $NaN0_2$ and a Corning 3–73. Fluorescence emission spectra were taken on all samples and by spectral

shape were seen to be that of DPH. By measurements with unlabeled samples and solvents, we conclude that background fluorescence or scattered light did not interfere in any of the measurements reported here. Because DPH is subject to quenching by dissolved oxygen, all solutions were purged for at least 10 min with argon or nitrogen prior to collecting fluorometric data.

Results

Homogeneous Solution Studies.

Figure 2 shows differential tangents for DPH in propylene glycol over a temperature range from –60 to +60 °C, observed with both a 10 and 30 MHz modulation frequency. The data shown on this figure are from two separate experiments conducted about 6 months apart but no attempt was made to distinguish the separate data sets since they were in precise agreement. Several points should be noted. The open circles and triangles represent the differential tangent observed with the excitation polarizer in the horizontal orientation and the emission polarizer varied from the vertical to the horizontal position in order to measure tan Δ. Clearly the data show that these values for tan Δ are zero at all temperatures. i.e., are zero irrespective of the rotational rate of the fluorophore. We conclude that the phase angle observed by this procedure of varying the emission polarizer is insensitive to the polarization of the fluorescence emission. Thus the observed differential tangents are the result of rotational motion of the fluorophore and are not significantly affected by any systematic errors in the instrumentation or phototube response. From the degree of scatter in the differential tangents we have estimated that these values are precise to ±0.008 at 30 MHz and ±0.004 at l0 MHz. These errors are equivalent to random error of about 0.05 ns in $\Delta\tau$ (tan Δ= ω$\Delta\tau$) at both 10 and 30 MHz. This degree of random error in $\Delta\tau$ remained constant throughout these experiments and was used in our analysis of errors. The differential tangent goes to zero at very low temperatures in the absence of rotational diffusion as predicted and observed by other researchers (Weber, 1977; Heldt, 1966; Jablonski, 1957; Spencer & Weber, 1970). Most importantly, the observed tan Δ_{max} values at both frequencies are in precise agreement with those predicted for an isotropic rotator with $r_0 = 0.390$ (Figure 2 and Table I). This result indicates that the depolarizing rotations of DPH in propylene glycol are isotropic and unhindered.

Figure 3 shows fluorescence lifetimes and steady-state anisotropy values for DPH in propylene glycol and in mineral oil. It is apparent from these data that our lifetime measurements are considerably less precise than the differential lifetimes (tangents) but this ought not to be surprising given the inherently more accurate data obtainable with differential methods. From the random error in the lifetime values in Figure 3, which contains two separate data sets, the accuracy of these measurements was ±0.5 ns. For the most part, the fluorescence lifetimes observed at 10 and 30 MHz are equivalent within experimental error, although there are some systematic differences at high temperatures where the lifetimes are short. In particular the lifetime at 10 MHz becomes smaller than the 30-MHz value. This phenomenon may be a result of the wavelength dependence of the time response of the phototubes, and the varying contribution of this effect at different lifetimes and frequencies. It should be noted that for lifetime measurements one measures the

difference in phase angle between the fluorescence emission and a scattering solution. Under the conditions of the present set of experi-ments, the phototube alternately observes light at 360 and 450 nm. In contrast, for differential measurements the photo-multiplier tubes always observe light of the same wavelength, and thus the measurements will in no way be affected by any wavelength dependence in the phototube response. Our final calculations of R and r_∞ are more sensitive to errors in tan Δ than in τ, so that the larger errors in rare not a concern in the interpretation of our data.

The data shown in Figures 2 and 3 provide measurements of τ, tan Δ, and *ras* a function of temperature for DPH in the isotropic solvents propylene glycol and mineral oil. As was described in the section on Theory, these values are adequate to obtain values for the rotational rate R. and for the limiting anisotropy (r_∞) at times which arc long compared with the fluorescence lifetime. In order to reduce the degree of scatter in the calculated values of R and r_∞, we utilized a smoothed data set for τ, tan Δ, and r for DPH in propylene glycol. This set was generated by drawing smooth lines through the measured quantities and reading off the necessary values at intervals of 5 °C. This smoothed data set was then used to calculate R and r_∞.

The rotational rates of DPH in propylene glycol obtained from steady-state anisotropy measurements (eq 5) are in precise agreement with those obtained from the hindered rotational model (eq 18 and Figure 4). Although not shown, the rotational rates obtained from the unhindered isotropic model (eq 10) also agree precisely with those shown in Figure 4; this ought not to be surprising since the equations for the hindered model reduce to those for an unhindered isotropic rotator when $r_\infty = 0$.

Smoothed data from Figures 2 and 3 were also used to obtain r_∞ as a function of temperature (Figure 5). These r_∞ values are equal to zero within experimental error, as would be expected since the unhindered isotropic model is adequate to describe the differential phase data in propylene glycol. However, below 10 °C the errors in the calculated values of r_∞ become quite large even with the smoothed data set. This is surprising in view of the fact that the tan Δ values are near their maximum and the steady-state fluorescence anisotropy is near 0.25, or 60% of its maximum value. The inaccuracy may derive from the sensitivity of r_∞ to errors in $\Delta\tau$ measurements; errors of ±0.05 ns are adequate to shift the r_∞ values to the dotted lines shown in Figure 5. Nonetheless, the data are sufficiently accurate for us to conclude that DPH behaves as a free isotropic rotator in propylene glycol.

DPH in Mineral Oil.

The differential tangents observed for DPH in mineral oil are shown in Figure 6. As for DPH in propylene glycol, tan Δ values with the polarizers crossed are zero, indicating no systematic errors in the measured values of tan Δ. The lowest attainable temperature was –6 °C, below which the mineral oil became turbid. At temperatures less than –2 °C microcrystals were visible in the sample, indicating local freezing of the mineral oil. As opposed to DPH in propylene glycol the tan Δ values did not reach the maximum value predicted by eq 11, and indicated by the solid bars on Figure 6. The percentage of tan Δ_{max} observed is 91 and 92 at 10 and 30 MHz, respectively (Figure 6 and Table I).

There are at least three possible causes for a failure to obtain the predicted value of tan Δ_{max}. These are (l) the rotations of the probe are hindered or (2) anisotropic and (3) the existence of a heterogeneous distribution of isotropic rotators. Since the absorption and emission axes lie along the long axis of DPH, and since DPH is an isotropic rotator in propylene glycol, it appears unlikely that DPH would behave as an anisotropic rotator in mineral oil. We used the tan Δ data in Figure 6 and the fluorescence lifetime and steady-state anisotropy data from Figure 3 to calculate R and r_{∞}. (In contrast to the data for propylene glycol, the raw data were utilized, not a smoothed data set.) The r_{∞} values so obtained are shown in Figure 7; r_{∞} becomes slightly positive below 10 °C and increases gradually to 0.055 and 0.022 at 30 and 10 MHz, respectively, at –6 °C. These nonzero r_{∞} values are outside our experimental error. (The error bars show the effects of errors 0.01 in r or 0.05 ns in r_{∞}) The errors in rare dominant at temperatures greater than 5 °C, and the errors in $\Delta\tau$ are dominant at temperatures lower than 5 °C. The hindered rotational model does not provide for any frequency dependence of the r_{∞} values; yet a significant frequency dependence was observed. As we previously noted, the sample contains microcrystals at temperatures below ca. –2 °C. We propose that the failure to obtain the predicted value of tan Δ_{max} is most likely a result of heterogeneous population of DPH molecules which is the result of a fraction of the DPH molecules being trapped within these “crystals”. It can be easily demonstrated that a fraction of the fluorescence population which is unable to rotate will result in both a decrease in tan Δ_{max} and an apparent nonzero value for r_{∞}.

The rotational rates of DPH in mineral oil obtained from both steady-state anisotropy measurements and the hindered rotational model are shown in Figure 8. At temperatures greater than 0 °C the rates calculated by both methods are in agreement to within our experimental uncertainties. At lower temperatures the rotational rates appear higher with the hindered rotational model, and the 30-MHz rates appear higher than those found at 10-MHz modulation frequency. This phenomenon results from nonzero r_{∞} value (see above), which translates into a higher apparent rotational rate for those molecules which can still undergo depolarizing rotations.

As for DPH in propylene glycol, we have concluded that DPH in mineral oil at temperatures greater than 10 °C is an isotropic rotator and that the nonideal behavior observed below this temperature is a result of partial freezing of the sample. In addition, these data indicate that differential polarized phase fluorometry, and the frequency dependence of the same, may be useful in determining whether a fluorophore is in a single homogeneous environment.

DPH in Saturated Phosphatidylchoines.

Differential tangents and fluorescence lifetimes of DPH in saturated phosphatidylcholines were determined over the temperature range 5–65 °C and at two modulation frequencies (10 and 30 MHz). Single bilayer vesicles of DMPC, DPPC, and DSPC were utilized.

The temperature profiles for tan Δ in all three lipids (Figures 10 and 11) are characterized by low values for tan Δ below T_c and a rapid increase of tan Δ at and around T_c, followed by a slow decrease in the differential tangent as the temperature further increases above the lipid transition temperature. (Note that the tan Δ values taken with the polarizers crossed are all near to zero.) The midpoints of these profiles (~24 °C for DMPC, ~41 °C for DPPC, and

~54 °C for DSPC) agree well with the T_c values reported by other authors (see Cullis, 1976, for summary of such data). Above T_c the magnitudes and slopes of the tan Δ profiles for the lipids appear to be identical, but in no case is the overall profile for tan Δ the typical symmetrical bell shape observed for DPH rotations in the isotropic solvents.

For all three phospholipids, at both frequencies, the tan Δ_{max} values fail to reach the maximum values predicted by eq 11 (see Table I). These tangent defects are in fact in excess of those predicted from Weber's theory for any degree of rotational anisotropy; Weber has, for example, calculated a maximum tangent defect of 25% for an infinitely anisotropic rotator. The data may, however, be readily fit by applying the theory of hindered rotations (Weber, 1978) whence tangent defects even larger than those observed by us may be readily accommodated.

Rotational rates (R) and r_∞ values (Figures 12 and 13) were obtained by applying the hindered rotational model to the differential phase data, the fluorescence lifetimes, and the steady-state anisotropies (Figure 9). From Figure 12 it is apparent that in all three phosphatidylcholines DPH is present in a highly hindered environment at temperatures < T_c and that a rapid increase in the rotational freedom (decrease in r_∞) occurs at T_c. In general, the values obtained at 10 and 30 MHz agree very well except in DMPC vesicles (Figure 12B) where small, but we think significant, differences do occur. Taken altogether, however, the fit to the data both qualitatively and quantitatively suggests the validity of applying the hindered rotation model to the motions of DPH in lipid bilayers.

The rotational rates for DPH in the saturated phosphatidylcholines obtained by application of the hindered rotational model are shown in Figure 13. At temperatures above T_c the rotational rates of DPH in all the lipids are similar as are the activation energies for DPH rotation (Table II). The reasonable equivalence of these values is in keeping with the approximately equal slopes of the tan Δ curves given in Figures 10 and 11. The rotational rates at temperatures < T_c are not shown because the inherent errors that appear under conditions where $r_\infty/r_0 > 0.7$ preclude accurate estimation of R. Figure 13 gives (as dashed lines) the confidence limits in R for errors in $\Delta\tau$ of ±0.05 ns and errors and errors in R of ±0.01, and it is immediately apparent how small random or systematic errors may readily result in major errors in the calculated rotational rates.

Despite these uncertainties in almost every experiment we observed an apparent decrease in R as the temperature is increased through the transition temperature. Representative data for DPPC at 10 MHz is shown (Figure 13). A similar effect was observed by Kawato et al. (1977). This decrease appears in all these phospholipids, and a gradual decrease in R with increasing temperature was also observed in DMPC bilayers which contain cholesterol. The studies of Veatch & Stryer (1977) have shown that a cholesterol content of up to 33 mol % does not decrease the rotational rate of DPH in liposomes of di(dihydrosterculoyl)phosphatidylcholine. Other studies in this laboratory have shown an increase in the collisional frequency of γ-hexachlorocyclohexane with carbazole-labeled phospholipids at temperatures below T_c (Lakowicz & Hogen, submitted for publication). Thus we are not inclined to dismiss the anomalous temperature dependence of R as being the result of systematic errors. Overall, however, the data show there to be no dramatic

changes in the rotational rate of DPH at the transition temperature in any of the lipid preparations in apparent contradiction of a typical assumption that has repeatedly been made on the basis of measurements of steady-state anisotropy. In addition, our results are in excellent agreement with those obtained using time-resolved methods (Table III).

DPPC-Ether.

The usefulness of the differential polarized phase fluorometric method for the study of probe motion in bilayer membranes may be well illustrated by studies of a system which behaves only slightly differently from those we have already described. The ether analogue of dipalmitoylphosphatidylcholine offered such a system since the change in the organization of the glycerol backbone region does not cause a major perturbation in the dynamic properties of the lipid (Schwarz & Paltauf, 1977). The tan Δ-temperature profile for DPH in DPPC-E is given in Figure 14C and indicates that the behavior of tan Δ in DPPC-E is similar to that observed in DPPC except that T_c is increased from about 41 °C to about 45 °C. Moreover, the temperature profile for r_∞ (Figure 17) and for a steady-state anisotropy plot (Figure 9B) also indicates an elevated transition temperature relative to DPPC. However, the rotational rates of DPH in DPPC-E and DPPC are similar at temperatures > T_c (Figures 13 and 18).

DMPC/Cholesterol. 3/1.

For vesicles composed of both DMPC and cholesterol in a 3 to 1 molar ratio, the differential tangents increased gradually with increasing temperature but the tan Δ values did not reach a maximum at any accessible temperature (Figure 15). Above 60 °C these vesicles ag-gregate. The limiting anisotropy decreases gradually with increasing temperature, but the depolarizing rotations remain hindered at all temperatures (Figure 16). The rotational rates of DPH are surprisingly rapid, being as fast or faster than that of DPH in DOPC or that of DPH in the saturated phosphatidylcholines above their transition temperatures (Figures 13 and 18). Our results are in agreement with those of Veatch & Stryer (1977) who observed rapid depolarization of DPH in cholesterol containing bilayers using time-resolved an· isotropy measurements.

DPH in Unsonicated Multilamellar Bilayers.

Distinct differences have been noted between the rotational behavior of DPH in multilamellar bilayers and those in vesicles (Lentz et al., l976a). These dissimilarities have been ascribed to the differences in radius of curvature and the sizes of the “cooperative units” in the two types of bilayered systems. Our data (Figure 9) employing measurements of steady-state anisotropy gave results similar to those of previous workers. The differential phase data reveal (Figures 14A and 14B) that, while the overall profiles for tan Δ vs. temperatures are similar in both types of bilayer, the unsonicated sample shows a sharper increase in tan Δ at T_c and that the tan Δ values are uniformly smaller in the unsonicated bilayers, the differences being most pronounced below T_c. Not surprisingly, r_∞ values calculated by application of the hindered rotation model also show a sharper transition profile (Figure 17). The pattern of behavior for R is essentially the same in the multilamellar and unilamellar vesicles (Table II) with R being subjected to the same degree of uncertainty at temperatures < T_c. Yet again, there is no evidence for a significant change in R as the lipid phase transition occurs.

DPH in DOPC.

The differential tangents of DPH in DOPC bilayers decrease with increasing temperature, except for a slight increase in tan Δ observed between 2 and 10 °C, at 30 MHz modulation (Figure 15). This region corresponds to the region where depolarizing rotations are of the proper mag-nitude to yield a maximum in tan Δ. At 10 MHz a maximum tan Δ is not observed, presumably because the rotations of DPH are too rapid even at 2 °C. At higher frequencies a higher rotational rate is required to obtain tan Δ_{max}· The maximum differential tangent observed in DOPC is much closer to the theoretical tan Δ_{max} than in any of the other bilayers we investigated (Table I). The hindered rotation theory indicates only a small limiting anisotropy which decreases with increasing temperature (Figure 16). The r_∞ values obtained at 30 MHz are larger than those obtained from the 10-MHz data, and these differences appear to be greater than our experimental uncertainties. In contrast, we may recall that for the case of the saturated phosphatidylcholines, and especially the DMPC/cholesterol mixture, there was excellent agreement between the values of r_∞ obtained at 10 and 30 MHz. It therefore appears that the hindered rotational model is less appropriate for DPH in DOPC bilayers. The calculated rotational rates of DPH in DOPC are linear at all temperatures and have activation energies of 6.9 and 5.7 kcal/mol, at 10 and 30 MHz, respectively (Figure 18). The data also indicate that because of the low limiting anisotropy for DPH in DOPC vesicles there is Jess uncertainty in the calculated R values.

Discussion

The data presented above quite clearly illustrate the value of differential phase fluorometry as a tool for investigation of the rotations of fluorophores in membranes. In the discussion that follows we will go into some detail regarding the technique and the interpretation of the data as they relate, on the one hand, to other approaches and, on the other hand, to the dynamic structure of a lipid bilayer.

Diphenylhexatriene possesses several spectral properties which make it a valuable fluorescence probe. It has a high extinction coefficient {Shinitzky & Barenholz, 1974) and the quantum yield approaches unity when the probe is dissolved in a hydrocarbon solvent. The fluorescence lifetime is about 11 ns in hydrocarbon solvents and varies to only a small extent with temperature (except in protic solvents such as propylene glycol). Although fluorescence yields are decreased in protic solvents relative to those observed in hydrocarbon solvents, spectra are not significantly shifted with respect to wavelength. The excitation polarization spectrum shows a broad region where (at –54 °C) r0 for the probe is 0.390 (vs. a maximum possible value of 0.4) and, in addition, the probe exhibits no significant emission anisotropy dependence on wavelength (Lakowicz & Prendergast, unpublished data). The broad separation of excitation and emission spectra means that there is little chance for depolarization by energy transfer and also that suitable excitation and emission wavelength may be chosen to minimize any problem due to Rayleigh or Raman scattering. Because of its minimal solubility in water, DPH is readily incorporated into the “hydrocarbon” phase of lipid bilayers. (Although the probe undergoes photobleaching we have not found this to be a major problem.)

As a result of these properties DPH has become a widely used probe for the estimation of membrane microviscosity. However, our data, as well as those of other workers (Kawato et al., 1977; Chen et al., 1977) have demonstrated that the steady-state anisotropies are determined primarily by the degree to which the rotations are hindered, and not by the probe's rotational rate. The degree to which a fluorophore's rotations are hindered is described by the cone angle θ_c (Kinosita et al., 1977) or the limiting anisotropy, r_∞. We feel it is important to stress and explain the meaning of these terms.

The cone angle θ_c is defined as the angle at which the DPH molecule encounters an infinite energy barrier. Using this assumed geometric constraint, Kinosita et al. (1977) obtained the following expression for the limiting anisotropy

$$r_\infty/r_0 = \left[(1/2)\cos\theta_0\left(1+\cos\theta_c\right)\right]^2 \tag{19}$$

Alternatively, this limiting anisotropy is related to the average angular distribution (θ) of the probe at times which are long compared with the fluorescence lifetime by

$$r_\infty/r_0 = \left(3\cos^2\theta - 1\right)/2 \tag{20}$$

We feel the latter interpretation of r_∞ is preferable because no assumptions are involved. Equation 20 relates r_∞ to the average angular distribution at long times, irrespective of the form of the barrier to rotational diffusion; θ is thus also observable experimentally. The former interpretation of r_∞ related this parameter to a unique and infinite energy barrier whose existence is not demonstrated by the experiment and therefore θ_c is meaningful only if the assumed infinite potential model is correct. The average angular distribution for complete depolarization ($r_\infty = 0$) is 54.74°. The corresponding cone angle is 90°.

Given the restricted depolarizing rotations of DPH, would other fluorophores be more suitable for the estimation of membrane microviscosities? It appears likely that a more spherical fluorophore would show greater similarities between these depolarizing rotations in solvents and bilayers than does DPH. However, in our opinion, a single fluorophore will never be completely satisfactory in this regard. The difficulty arises, not because the depolarizing rotations will always be different in solvents and membranes, but rather because the value of the microviscosity obtained will be critically dependent upon the method used in its estimation. There is no reason to assume that the environment of a lipid bilayer will provide the same viscous drag on lateral diffusion of fluorophores, rotational diffusion of fluorophores, passive transport of ions, and diffusion of small molecules such as water and oxygen. To further illustrate this point. in the following paper (Lakowicz et al., 1979) we have calculated the microviscosity of DMPC bilayers from steady-state anisotropies of DPH and from the diffusivity of molecular oxygen. Below the transition temperature these values are 50 and 0.3 P, respectively. It is not necessary to choose between these values, or to attempt to form an average. Rather, we must recognize that lipid bilayers cannot be characterized by a single microviscosity. Because of these considerations, we feel it is misleading to report fluorescence anisotropy data in terms of microviscosity.

Harmonic methods such as we have utilized are frequently criticized because a single exponential decay is assumed. For several reasons we feel a harmonic method is suitable in this case. Firstly, as observed by time-resolved methods, the decays of DPH fluorescence intensity are well represented by a single exponential (Kawato et al., 1977). Throughout these experiments we observed good agreement between the lifetimes measured by the phase shift and the demodulation method. and good agreement between 10 and 30 MHz data. The maximum difference we observed between these four measurements of the fluorescence lifetime was 1.7 ns, this observation being made in DMPC bilayers which also contained cholesterol. These differences, when propagated into final values for R and r_∞ do not significantly alter our conclusions. The decays of the fluorescence anisotropy of DPH in bilayers is frequently described as being nonexponential. However, a more correct description might be to describe these decays as being a single exponential plus a constant term. The theory described in eq 12 through 18 is completely appropriate in this case. The agreement between 10- and 30-MHz data lends further support to this view. Finally. there is excellent agreement between our data and those obtained by pulse fluorometry (Kawato et al., 1977) with respect to values of r_∞ and rotational rates (Table III).

The advantages of the harmonic method should be indicated. At a single temperature, τ, $\Delta\tau$, and r may be measured in about 2 min and these in turn may be used to calculate R and r_∞ Consequently, a complete temperature profile for R and r_∞ in a given bilayer may be determined at two frequencies in about 8 h, the most time-consuming step being equilibration at each new temperature.

One intriguing aspect of this work is the similar profile for tan Δ below and above T_c (Figures 10 and 11). The tan Δ_{max} values are governed by the decrease in r_∞ at the transition temperature, and not by the fluorophore's rotational rate. One is tempted to speculate that the DPH molecules change their average environment at the transition temperature, for example, a relocalization from the carboxyl end to the methyl end of the acyl side chains. However, if the localization of the fluorophore were temperature dependent, we might expect DPH to have different affinities for bilayers in the solid and liquid states. The partition coefficient between saturated phosphatidylcholines which are above and below their transition temperatures is near unity (Lentz et al., 1976b). Thus it appears unlikely that alterations in fluorophore localization are the source of the alterations in r_∞. The question remains as to why such values of r_∞ exist, and at present we simply do not know.

In summary, by the combined use of both differential phase and steady-state polarization measurements we demonstrated a fundamental difference in the depolarizing rotations of DPH in solvents and in lipid bilayers. Caution must be used in the interpretation of anisotropy measurements in terms of membrane microviscosity.

Acknowledgments

Our special thanks go to Professor Gregorio Weber for providing us with the differential phase theory for fluorophores in a hindered environment prior to its publication. Additionally, we thank the Freshwater Biological Research Foundation, and especially its founder, Mr. Richard Gray, Sr., without whose assistance this work would have been impossible. We are also indebted to Mrs. Evonne Webster for indefatigable efforts expended in preparation of this manuscript. Finally, we thank Mrs. Luanne Wussow for preparing all of the figures.

These studies were supported by National Institutes of Health Grants ES 01283 (to J.R.L.) and CA 15083 (to F.G.P.), American Heart Association Grant 76–706 (to J.R.L.), and a grant from the Muscular Dystrophy Association (MDA-24) (to F.G.P.). This work was done during the tenure of an Established lnvestigatorship (to J.R.L.) of the American Heart Association. A preliminary account of this work was presented at the Discussions of the Biophysical Society, Airlie, VA, April 1978.

References

Chen LA, Dale RE, Roth S, & Brand L. (1977) J. Biol. Chem 252, 2163. [PubMed: 849925]

Cogan U, Shinitzky M, Weber G, & Nishida T. (1973) Biochemistry 12, 521. [PubMed: 4683495]

Cullis PR, De Kruijiff B, McGrath AE, Morgan CG, & Radda GK, (1976) in Structure of Biological Membranes (Abrahamsson S, & Pascher I, Eds.) p 389, Plenum Press, New York.

Dale RE, Chen LA, & Brand L. (1977) J. Biol. Chem 252, 7500. [PubMed: 914824]

Heidt J. (1966) Acta Phys. Pol 15, 3.

Jablonski A. (1957) Acta Phys. Pol 16, 471.

Jablonski A. (1965) Acta Phys. Pol 28, 717.

Kawato S, Kinosita K Jr., & Ikegami A. (1977) Biochemistry 16, 2319. [PubMed: 577184]

Kinosita K, Kawato S, & Ikegami A. (1977) Biophys. J 20, 289. [PubMed: 922121]

Lakowicz JR, & Prendergast FG (1978a) Science 200, 1399. [PubMed: 663620]

Lakowicz JR, & Prendergast FG (1978b) Biophys. J 24, 213. [PubMed: 708824]

Lakowicz JR, Prendergast FG, & Hogen D. (1979) Biochemistry 18 (following paper in this issue).

Lawaczeck R, Kainosho M, & Chan SI (1976) Biochim. Biophys. Acta 443, 313. [PubMed: 963059]

Lentz B, Barenholz Y, & Thompson TE (1976a) Biochemistry 15, 4521. [PubMed: 974073]

Lentz B, Barenholz Y, & Thompson TE (1976b) Biochemistry 15, 4529. [PubMed: 974074]

Mantulin WW, & Weber G. (1977) J. Chem. Phys 66, 4092.

Perrin F. (1936) J. Phys. Radium 7, 1.

Schwarz FT, & Paltauf F. (1977) Biochemistry 16, 4335. [PubMed: 911757]

Shinitzky M, & Barenholz Y. (1974). J. Biol. Chem 249, 2652. [PubMed: 4822508]

Shinitzky M, Dianoux AC, Gitler C, & Weber G. (1971) Biochemistry 10, 2106. [PubMed: 4104937]

Spencer RD, & Weber G. (1969) Ann. N.Y. Acad. Sci 158, 361.

Spencer RD, & Weber G. (1970) J. Chem. Phys 52, 1654.

Veatch WR, & Stryer L. (1977) J. Mol. Biol 117, 1109. [PubMed: 606835]

Weber G. (1977) J. Chem. Phys 66, 4081.

Weber G. (1978) Acta Phys. Pol. A 54, 173.

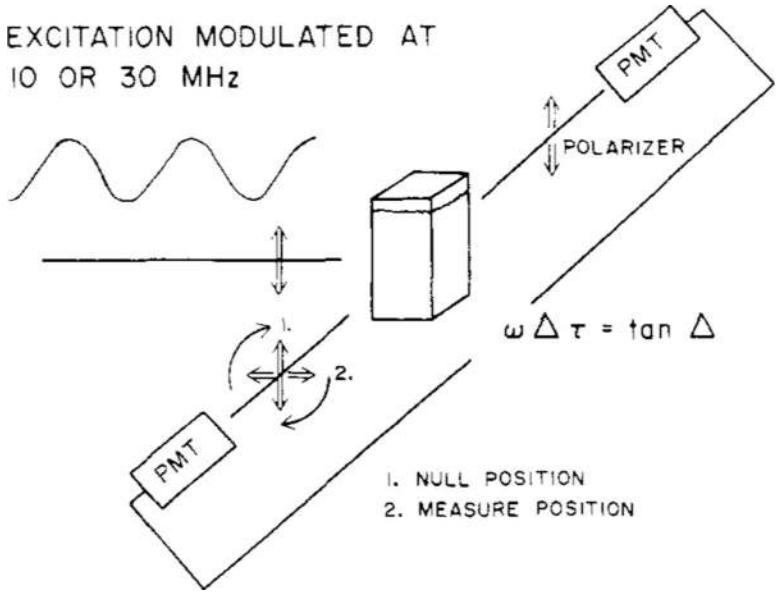

FIGURE 1:
Schematic of a differential phase fluorometer.

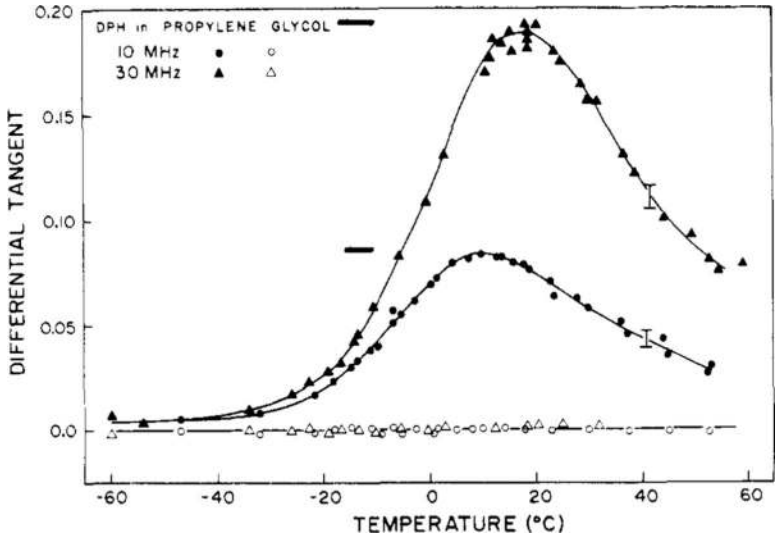

FIGURE 2:

Differential tangents of DPH in propylene glycol. The solid dots represent the differential tangents at the frequencies indicated, and the open dots represent the tangent value observed when the excitation polarizer is horizontal, and hence orthogonal to both emission polarizers irrespective of their orientation. This figure contains data from two separate experiments. The solid bars indicate the theoretical tan Δ_{max} for an isotropic rotator with $r_0 = 0.390$ and $\tau = 5.0$ and 4.3 ns at 10 and 30 MHz, respectively; [DPH] = 5 X 10^{-6} M.

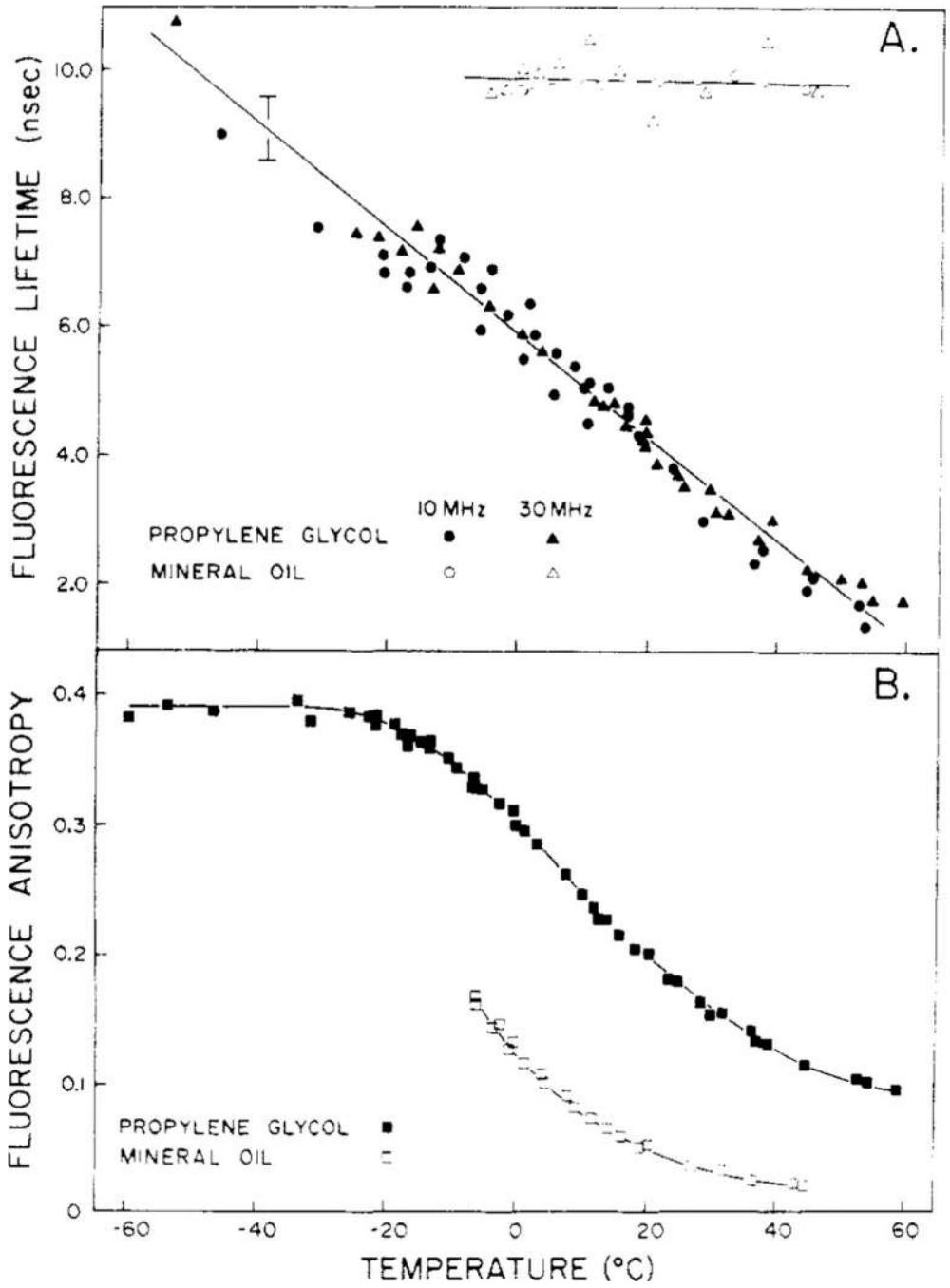

FIGURE 3:

Fluorescence lifetimes and steady-state fluorescence anisotropies of DPH in propylene glycol and mineral oil. This figure contains data from two separate experiments.

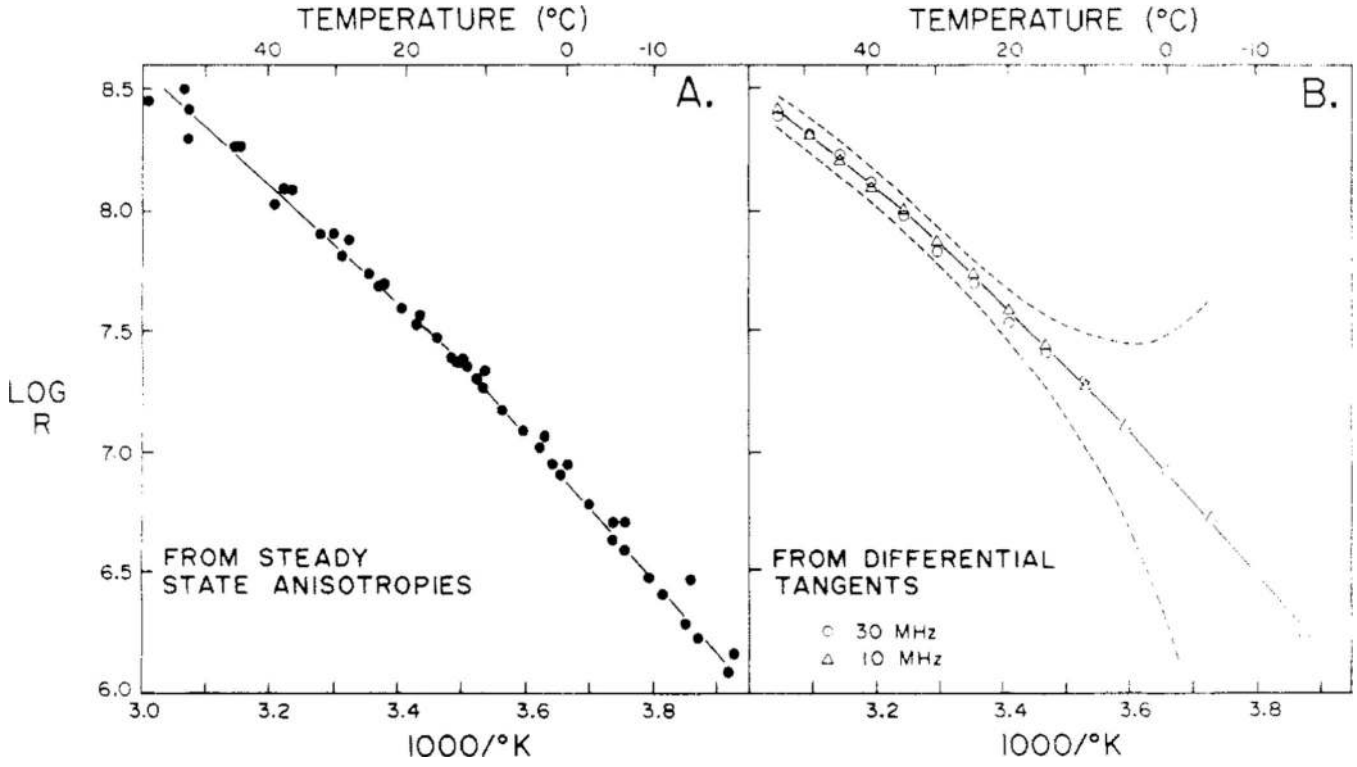

FIGURE 4:

Rotational rates of DPH in propylene glycol. Rotational rates for DPH were obtained from steady-state fluorescence anisotropies (A) and from the hindered rotational model (B), using both 10- and 30-MHz data. In order to minimize scatter in the *R* values obtained from the hindered rotational model, we use a smoothed data set obtained from reading the required values of τ, tan Δ and *r* off the lines drawn through the data points on Figures 2 and 3. The dashed line shows the errors in the calculated *R* values which result from errors of ±0.5 ns in τ, ±0.05 ns in $\Delta\tau$ and ±0.01 in *r*.

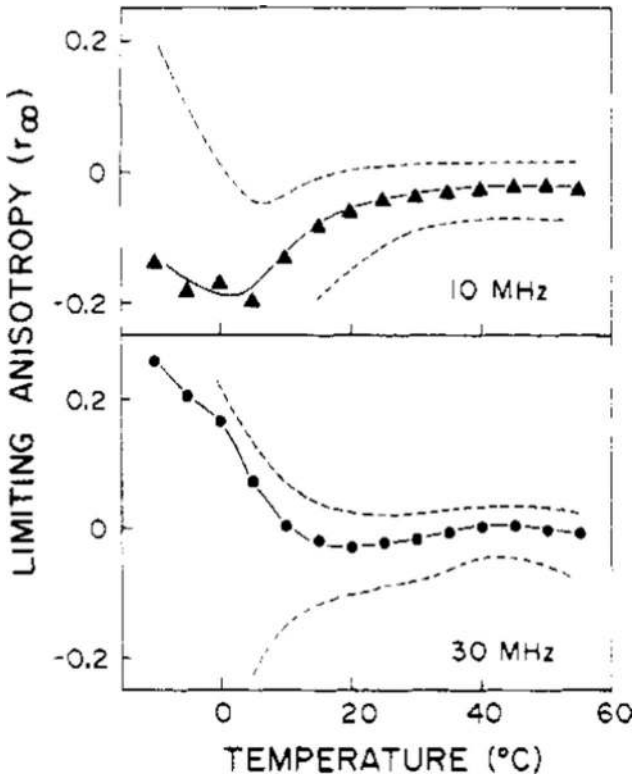

FIGURE 5:

Limiting anisotropies for DPH in propylene glycol obtained from the hindered rotational model. The smoothed data for DPH in propylene glycol was used. The dashed lines represent the errors in the calculated r_∞ value resulting from error of ±0.5 ns in τ, ±0.05 ns in $\Delta\tau$, and ±0.01 in r. The major contributions to the error are in $\Delta\tau$.

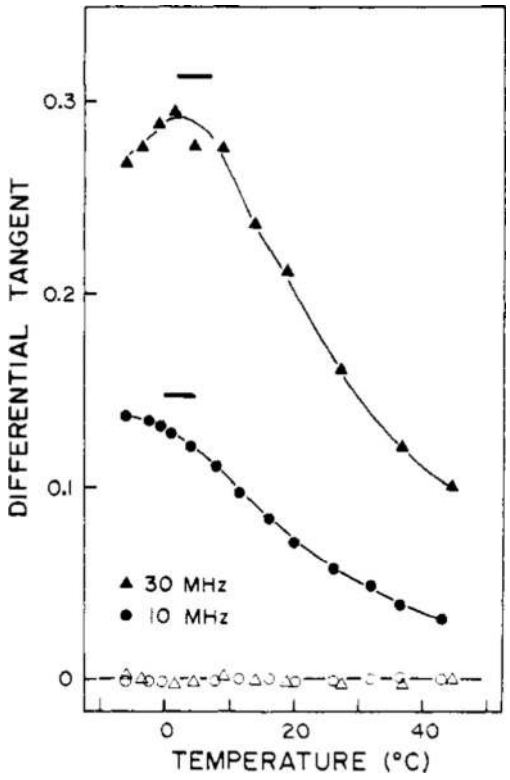

FIGURE 6:

Differential tangents for DPH in mineral oil. The solid dots indicate the differential tangents, and the open dots represent the differential tangent observed when the excitation polarizer is horizontal. The solid horizontal bars indicate tan Δ_{max} for an isotropic rotator with r_0 = 0.390 and τ = 9.9 ns; [DPH] = 5×10^{-6}M.

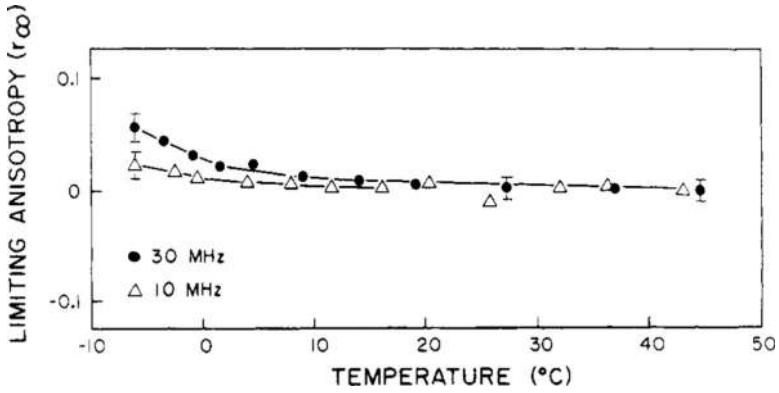

FIGURE 7:

Limiting anisotropies of DPH in mineral oil obtained from the hindered rotation model. The error bars indicate the effect of ±0.05 ns in $\Delta\tau$ and ±0.01 in r. The errors in r dominate above 5 °C, and the errors in $\Delta\tau$ dominate below 5 °C.

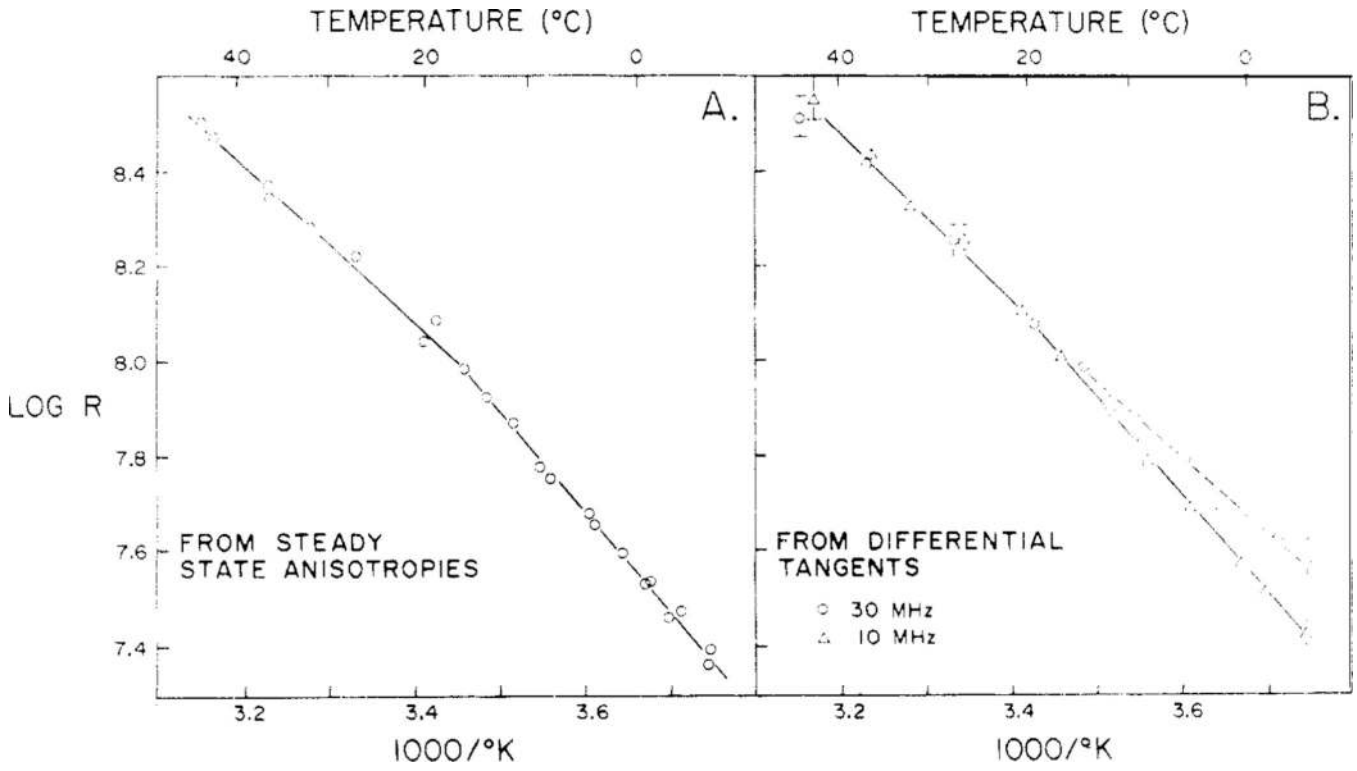

FIGURE 8:

Rotational rates for DPH in mineral oil obtained from steady-state anisotropies and the hindered rotational model. The raw data were used, and not smoothed data as were used for propylene glycol. The error bars indicated ±0.05 ns in $\Delta\tau$.

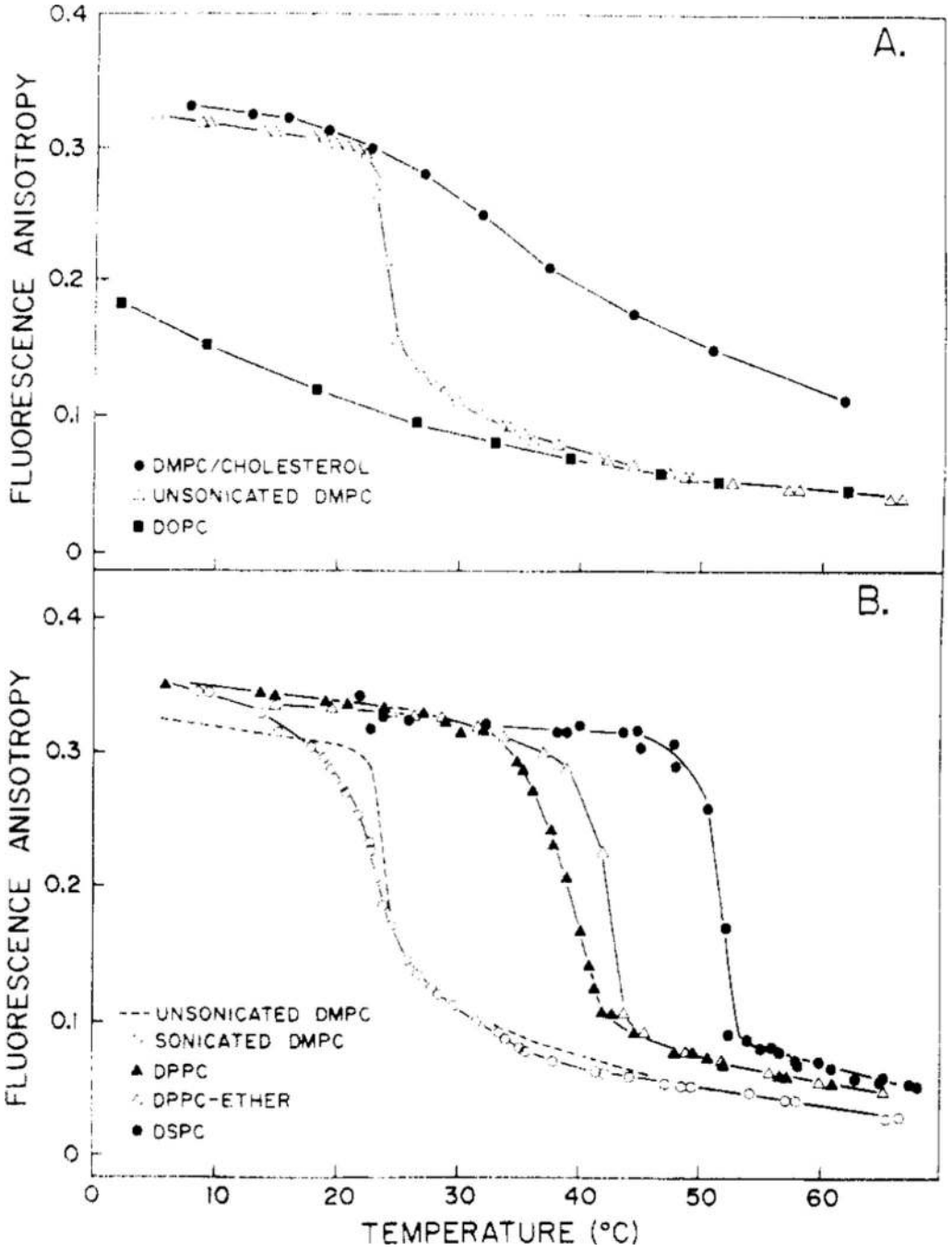

FIGURE 9:
Steady-state fluorescence anisotropies of DPH in the lipid bilayers used in these studies.

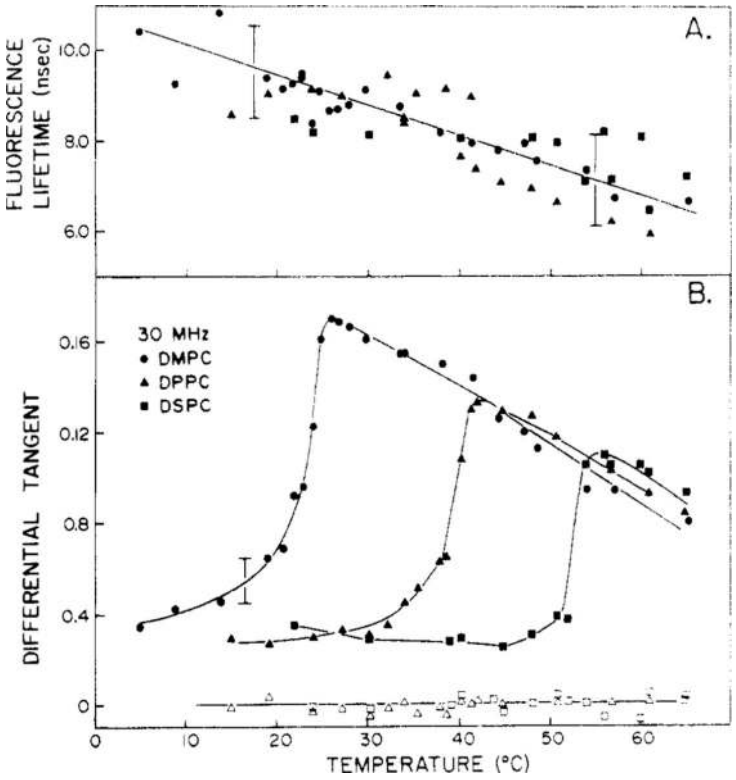

FIGURE 10:

Differential tangents and fluorescence lifetimes of DPH in vesicles composed of saturated phosphatidylcholines, 30 MHz. The open symbols represent the crossed polarizer data for the lipid represented by the same closed symbols. The data for DMPC are from two separate vesicle preparations. Measurements were made at 30 MHz; solid circles represent DMPC, solid triangles, DPPC, solid squares, DSPC.

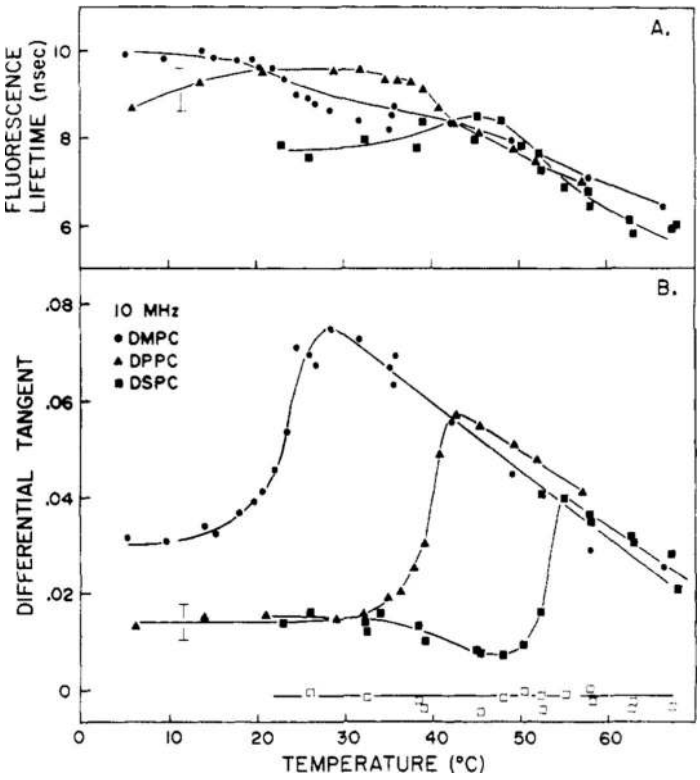

FIGURE 11:

Differential tangents and fluorescence lifetimes of DPH in vesicles composed of saturated phosphatidylcholines, 10 MHz. The open squares represent the crossed polarizer data for DSPC vesicles. The figure contains data from two separate vesicle preparations of DMPC.

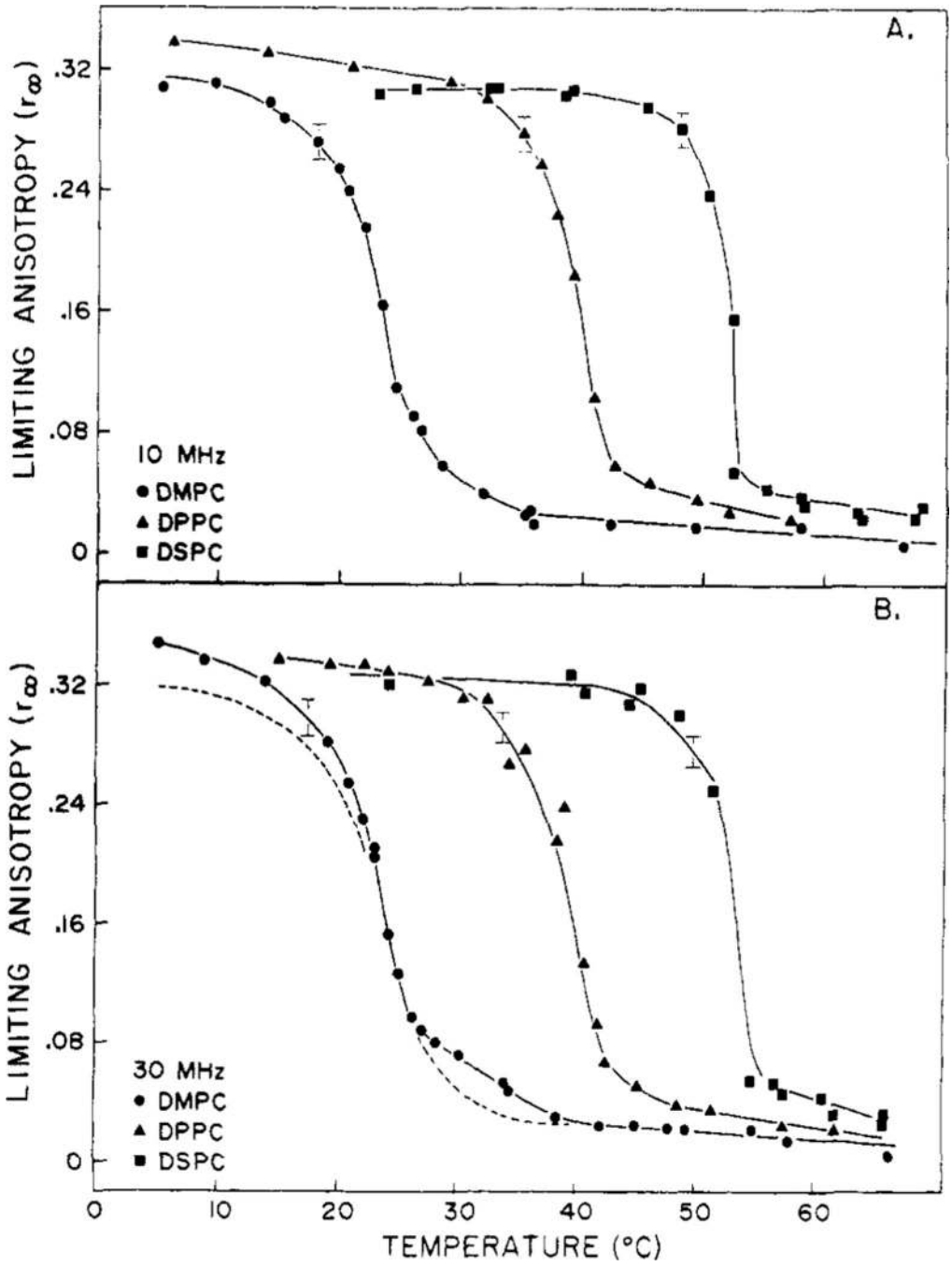

FIGURE 12:

Limiting anisotropies (r_∞) of DPH in vesicles composed of saturated phosphatidylcholines. Data are shown for 10 (A) and 30 MHz (B). The dashed line in part B represents the r_∞ values observed at 10 MHz. The errors in r_∞ are relatively constant with temperature. Below the transition temperature, errors in $\Delta\tau$ dominate, and above this temperature the errors in r are dominant.

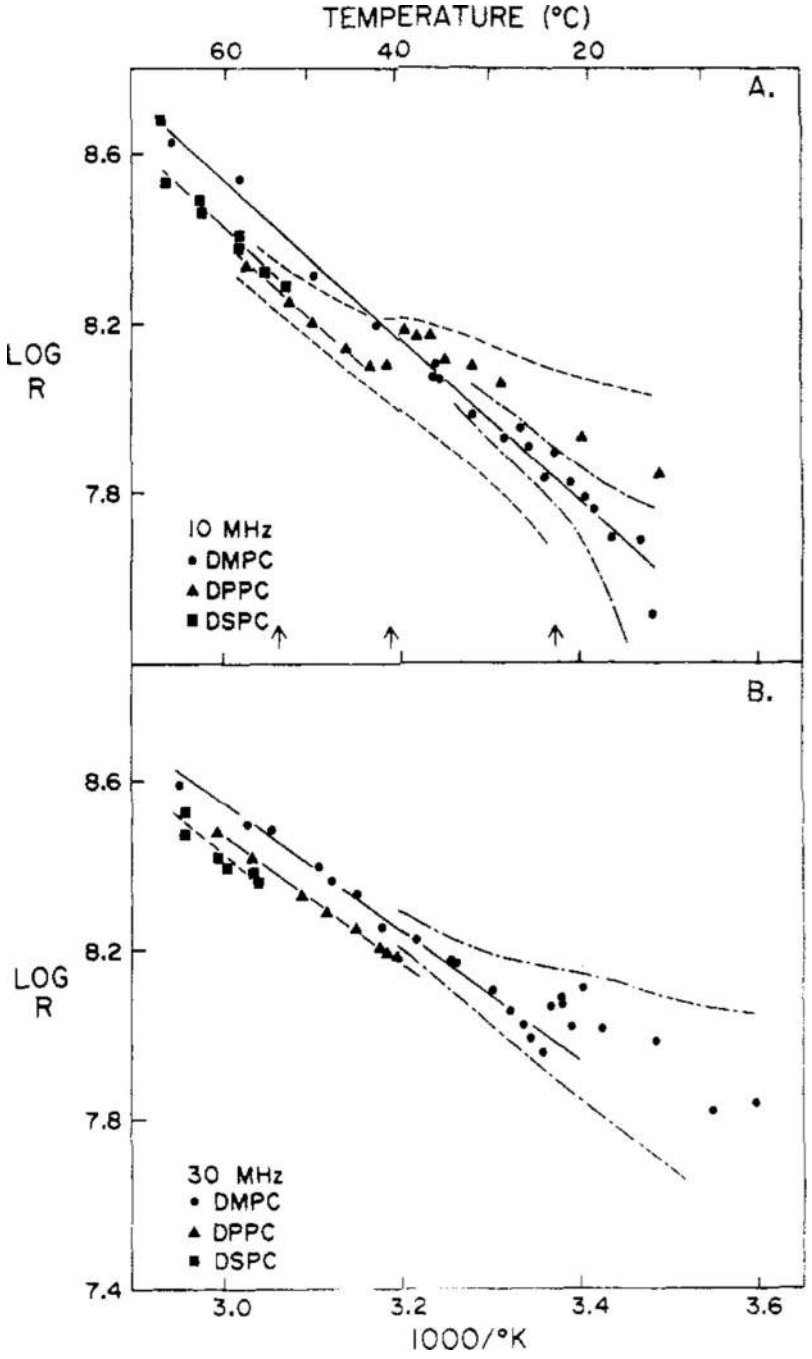

FIGURE 13:

Rotational rates of DPH in saturated phosphatidylcholine vesicles. Data are shown for 10 (A) and 30 MHz (B). The dashed lines on part A represent the errors in the calculated value of R for DPH in DPPC (---) and in DMPC (-·-·-) resulting from errors of ±0.05 ns in $\Delta\tau$, Variations in R almost as large would result from errors in $r = \pm 0.01$. The rotational rates at temperatures below T_c or not shown due to the large experimental uncertainty. The arrows indicate the temperature at which the r_∞ value has decreased through one-half of the maximum observed change.

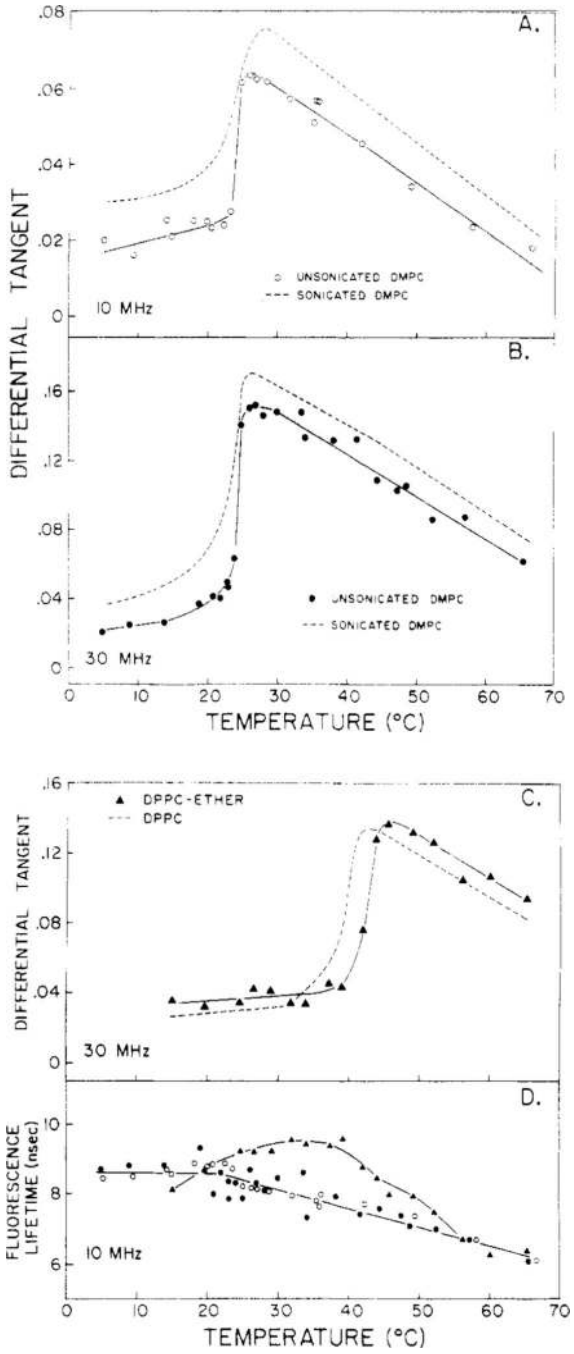

FIGURE 14:

Differential tangents and fluorescence lifetimes for single bilayer and multilamellar bilayers of DMPC and DPPC-ether. (A) Multilamellar DMPC bilayers (○) and comparative data for single lamellar bilayers (---) at 10 MHz. (B) Same as A, except at 30 MHz (●). (C) Single lamellar bilayers of DPPC-ether (▲) and comparative data for DPPC (---). (D) Fluorescence lifetimes.

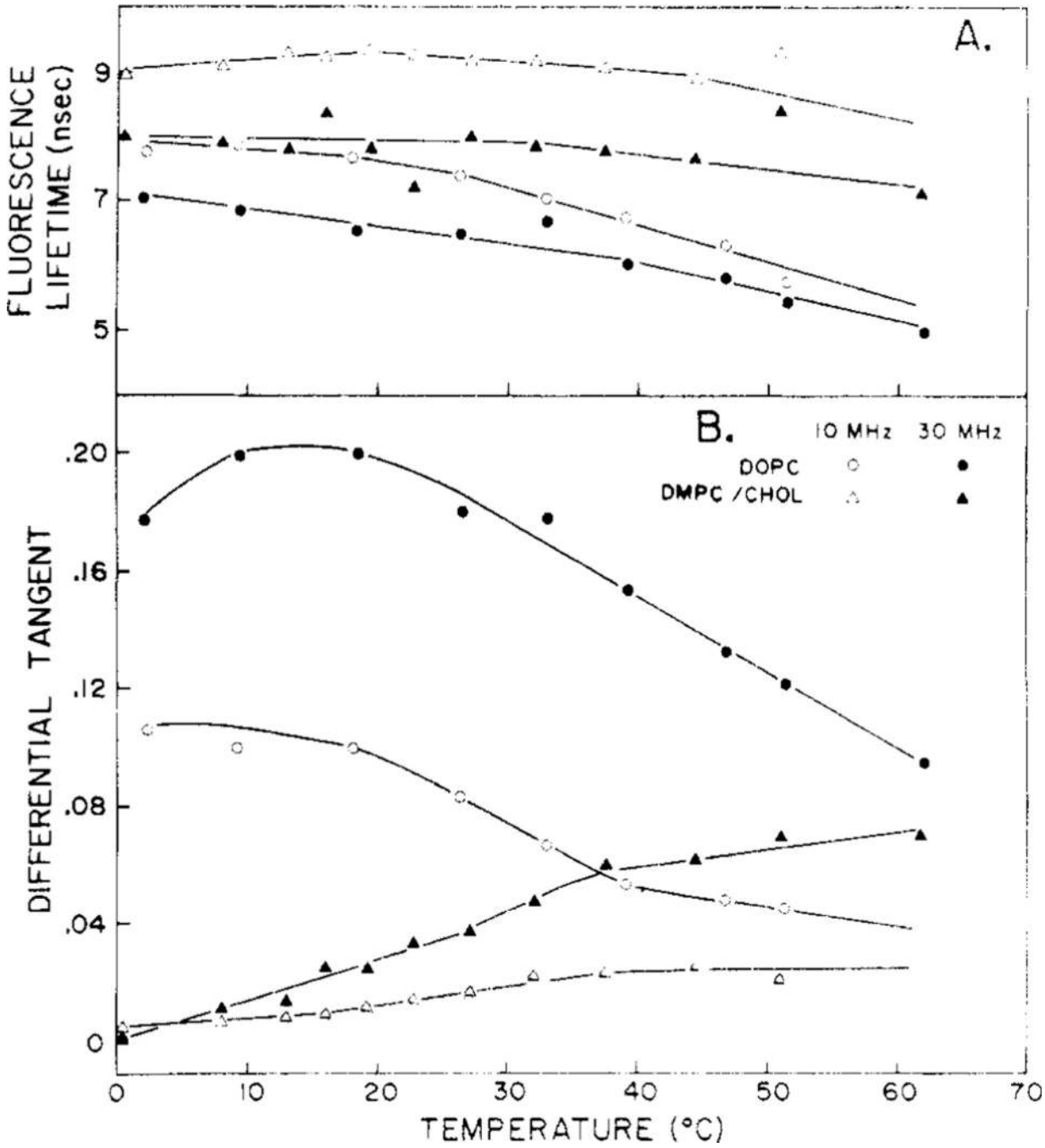

FIGURE 15:
Differential tangents and fluorescence lifetimes for DPH in vesicles of DOPC and DMPC/cholesterol, 3/1.

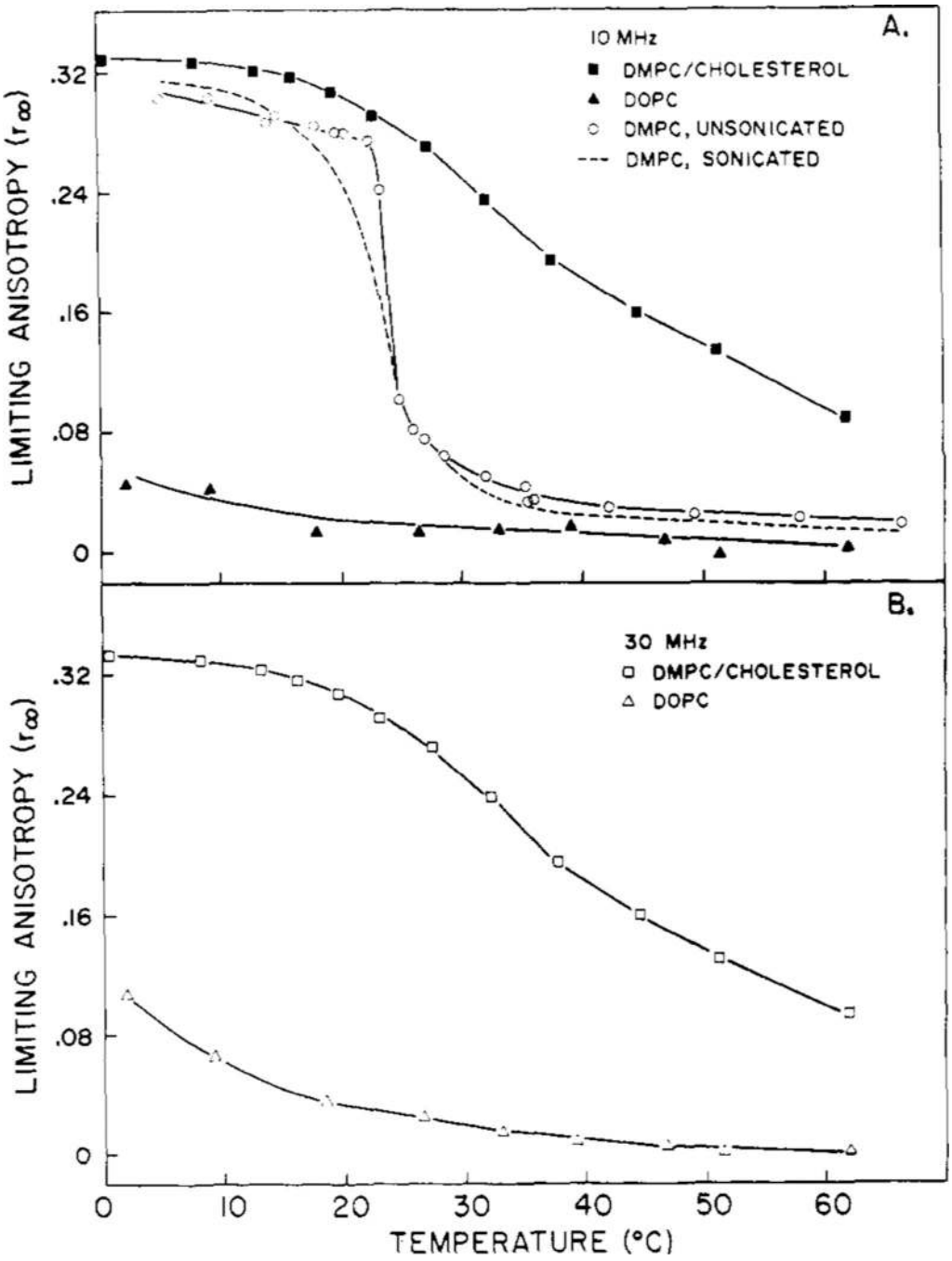

FIGURE 16:
Limiting anisotropies of DPH-labeled lipid bilayers.

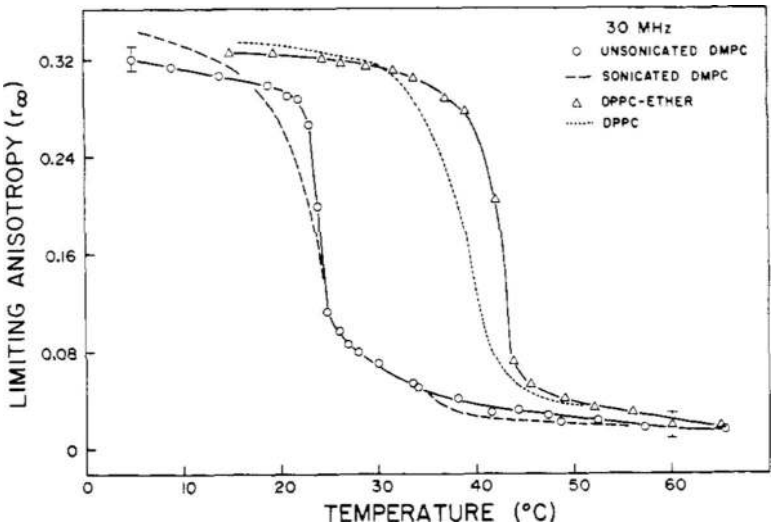

FIGURE 17:

Limiting anisotropies of DPH-labeled lipid bilayers. Error bars show uncertainty in r_∞ resulting from ±0.01 in r. This error is relatively constant across the r_∞ temperature profile.

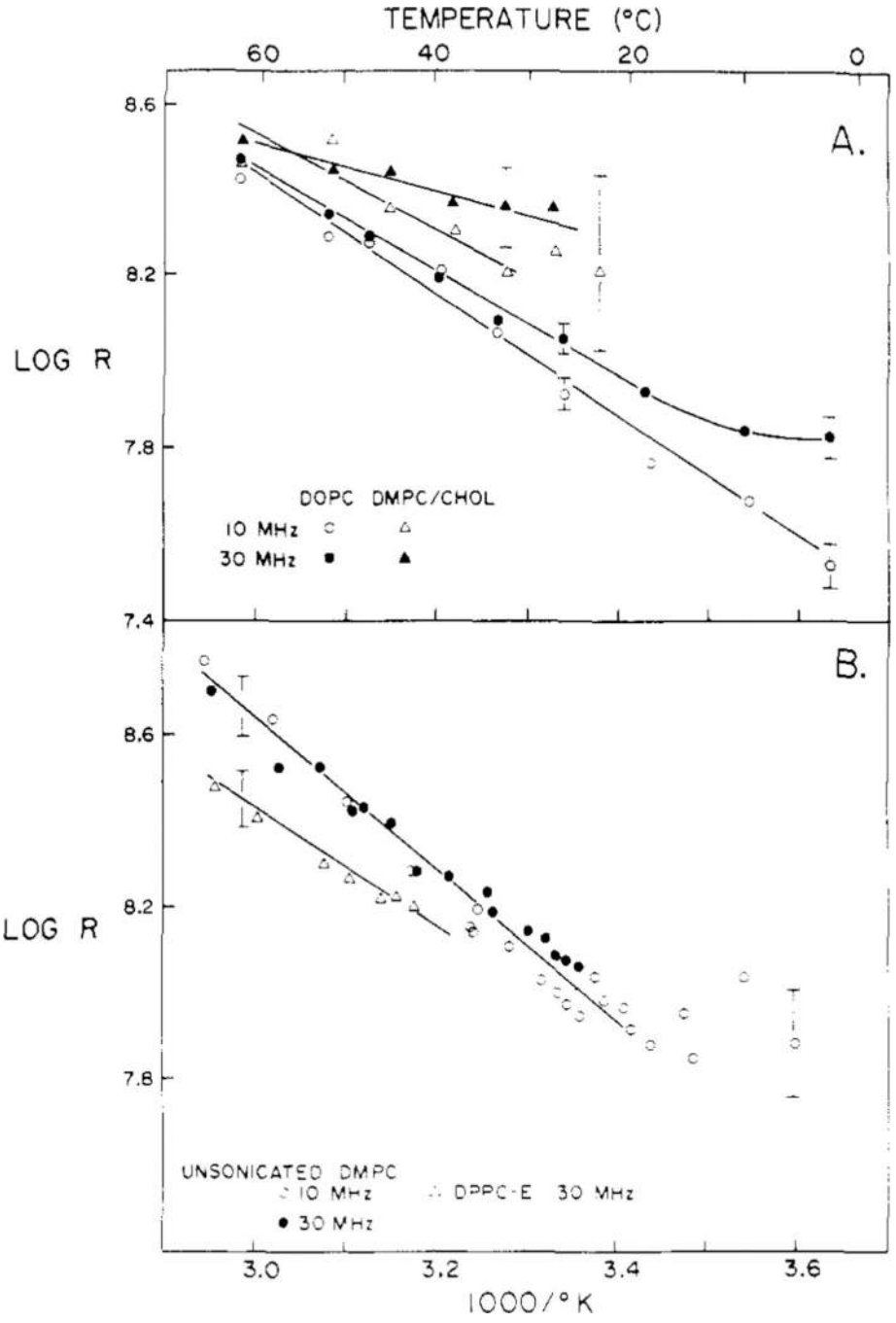

FIGURE 18:
Rotational rates of DPH in lipid bilayers.

Table I:

Maximum Differential Tangents for DPH in Solvents and in Lipid Bilayers

sample	frequency (MHz)	temp (°C)[a]	τ (ns)[b]	tan Δ_{max} obsd	tan Δ_{max} calcd[c]	% of theory
mineral oil	10		9.9	0.136[d]	0.150	91
	30	2	9.9	0.292	0.318	92
propylene glycol	10	10	5.0	0.082	0.081	101
	30	19	4.3	0.185	0.195	95
DOPC	10		7.7	0.105	0.127	83
	30	14	6.9	0.200	0.274	73
DMPC[e]	10	26	8.5	0.073	0.132	62
	30	27	8.5	0.170	0.298	52
DMPC[f]	10	28	8.8	0.084	0.136	68
	30	26	8.7	0.188	0.302	62
DPPC	10	43	8.1	0.057	0.131	43
	30	42	7.1	0.133	0.267	50
DSPC	10	55	7.2	0.040	0.113	35
	30	56	7.5	0.110	0.277	45
DMPC/	10		8.8	0.025[g]	0.135	19
cholesterol	30		7.9	0.068[g]	0.288	24
(3/1)						
DPPC-ether	30	46	8.1	0.137	0.289	47

[a] Temperature at the maximum differential tangent.

[b] Fluorescence lifetime observed at the temperature of the maximum tangent (eq 11).

[c] For an unhindered isotropic rotator (eq 11).

[d] This value may not represent the true maximum because a lower temperature could not be obtained with crystallization of the solvent (see Figure 6).

[e] Unsonicated multilamellar bilayers.

[f] Sonicated single lamellar bilayers. All the following bilayers are also sonicated.

[g] At the highest temperature used, 63 °c, the vesicles aggregated and the tan Δ appeared to still be increasing (Figure 15B).

Table II:

Activation Energies for the Rotational Rates[a] of DPH in Lipid Bilayers[b] and in Isotropic Solvents

	E_a(kcal/mol)[c]	
sample	**10 MHz**	**30 MHz**
mineral oil	7.4 ± 0.7	7.4 ± 0.7
propylene glycol[d]	11.4 ± 1.5	11.5 ± 1.6
DOPC	6.9 ± 0.5	5.7 ± 0.5
DMPC (sonicated)	8.7 ± 1.0	6.8 ± 0.8
DMPC (unsonicated)	9.3 ± 0.7	7.2 ± 1.2
DPPC	8.1 ± 3.0	7.2 ± 4.0
DMPC/cholesterol, 3/1	4.9 ± 4.0	2.6 ± 2.5
DPPC-ether		6.6 ± 1.8

[a] Rotational rates were obtained from the hindered rotational model.

[b] Unless otherwise indicated, ail bilayers are unilamellar sonicated vesicles.

[c] These activation energies refer to temperatures above T_c. The errors indicate the maximum range consistent with the errors in $\Delta\tau = \pm 0.05$ ns and in $r = \pm 0.01$.

[d] The smoothed data set was utilized.

Table III:

Comparison of R and r_∞ for DPH in DPPC Vesicles as Observed by Differential Polarized Phase Fluorometry and Time-Resolved Anisotropy Measurements

		phase fluorometry	
temp (°C)	time resolved[a]	10 MHz	30 MHz
	Limiting Anisotropy		
20	0.32	0.32	0.33
40	0.13	0.16	0.14
60	0.03	0.03	0.02
	Relaxation Time (ns)[b]		
40	1.3	1.1	1.1
50	1.0	1.1	0.7
60	0.7	0.8	0.6

[a] Kawato et al., 1977.

[b] $(6R)^{-1}$.